

# Graphical Solution of Turbulent-flow Diffusion Equations

P. A. LONGWELL

California Institute of Technology, Pasadena, California

Linear partial-differential equations are often encountered when thermal or material diffusion in flowing systems is considered. Analytic solutions of such equations are known for only the simplest situations. In two examples a graphical method of solution is presented and demonstrated which makes feasible, without excessive labor or special computing facilities, the use of available knowledge concerning turbulent flow in the prediction of thermal or material transfers in complex situations involving linear steady flow.

Prediction of the distribution of temperature or concentration in flowing streams is of interest in industrial applications. In recent years studies of turbulence have led to means of estimating eddy properties (4), which permit the solution of differential equations, at least in principle, to yield the desired information for any particular situation. In practice the solution of differential equations involving eddy properties has proved difficult, but a straightforward and relatively easy method of obtaining solutions of certain types of differential equations which apply to heat transfer and material transfer in flowing streams has been devised.

## DIFFERENTIAL EQUATIONS FOR THERMAL AND MATERIAL TRANSPORT

If there is thermal transport between the parallel plates shown in Figure 1 and a fluid which is flowing turbulently between them, the over-all energy balance may often be expressed accurately by the equation

$$u_x \frac{\partial T}{\partial x} = \frac{\partial}{\partial y} \left[ \epsilon_{cy} \frac{\partial T}{\partial y} \right] \quad (1)$$

when the eddy conductivity in the  $y$  direction is defined (4) by the relation

$$\epsilon_{cy} = \epsilon_{cy} + K = \frac{-\dot{Q}_y}{\sigma C_p \left( \frac{\partial T}{\partial y} \right)} \quad (2)$$

In the derivation of Equation (1) it is assumed that conditions are steady and that the velocity is a function only of the  $y$  coordinate. It is further assumed that the specific heat and weight of the fluid are constant, that there are no temperature gradients in the  $z$  direction, and that there are no energy sources in the fluid. Changes in potential and kinetic energy, viscous dissipation, and conduction in the  $x$  direction are neglected.

For thermal transport in a fluid flowing through a circular section of constant diameter, assumptions analogous to those made above lead to the relationship

$$ru_x \frac{\partial T}{\partial x} = \frac{\partial}{\partial r} \left( r \epsilon_{cr} \frac{\partial T}{\partial r} \right) \quad (3)$$

Turbulent diffusion may be described by use of an eddy diffusivity defined in the  $y$  direction, for example, by the equation

$$\epsilon_{dky} = \epsilon_{dky} + D_{ky} = \frac{c_k u_y - \dot{m}_{ky}}{\frac{\partial c_k}{\partial y}} \quad (4)$$

in which  $u_y$  is the hydrodynamic velocity of the fluid in the  $y$  direction. Equation (4) is an extension of the relationships of Opfell and Sage (15).

Simplifying assumptions, which are often appropriate, give differential equations for turbulent diffusion that are similar to Equations (1) and (3) but

have  $c_k$  substituted for  $T$  and  $\epsilon_{dk}$  in place of  $\epsilon_c$ .

## GENERAL FORM OF SIMPLIFIED DIFFERENTIAL EQUATION

If it is assumed that the eddy conductivity and diffusivity are functions only of the coordinate normal to the direction of flow, Equations (1) and (3) and the analogous ones for material transport are all of the form

$$\frac{\partial \phi}{\partial x} = f_1(y) \frac{\partial}{\partial y} \left[ f_2(y) \frac{\partial \phi}{\partial y} \right] \quad (5)$$

The coordinate  $y$  in Equation (5) is generalized to include the radial coordinate for cylindrical symmetry. While the eddy properties are probably functions of variables other than this one coordinate, the approximation seems adequate in view of the present state of knowledge regarding these eddy properties.

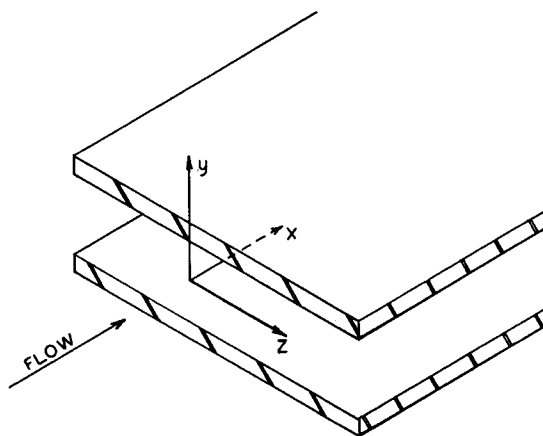


Fig. 1. Flow between parallel plates.

Equation (5) is a linear partial-differential equation but is not susceptible to analytic solution except in the simplest situations. For the case of plug flow with constant conductivity or diffusivity, the solutions are analogous to those for transient heating or cooling of a solid, given by Carslaw and Jaeger (3) for both the infinite slab and infinite cylinder for a variety of boundary conditions. Graetz (5) found the solution for plug flow in a pipe with uniform wall temperature and (6) also found a series-expansion analytic solution for the case of laminar flow with parabolic velocity distribution in a pipe with uniform wall temperature; this solution is given by Jakob (7). Berry (1) obtained formal solution to Equations (1) and (3) as an infinite series of solutions to a Sturm-Liouville problem, but for any specific instance these solutions must be obtained by lengthy numerical computations. Butler and Plewes (2) found a series solution for the case of diffusion in laminar flow between parallel plates. However even the analytic solutions for laminar flow with simple boundary conditions are very complicated, and it becomes necessary to find better methods for the solution of more complex problems.

Numerical methods have been applied to heat transfer with streamline flow by Norris and Streid (14), Kays (8), Schenk (19), and others. The use of electrical analogy to solve the turbulent heat transfer problem between parallel plates has been described by Schlenger et al. (16). Schmidt (17) described a graphical method for the solution of transient-heat-conduction problems in solids, which was extended to cylindrical and spherical bodies by Nessi and Nisolle (13). This method is described by McAdams (11), Jakob (7), and many others. Later Schmidt (18), in a paper which did not become well known in this country, described a graphical method for solution of partial-differential equations of the type shown in Equation (5). Schmidt's method, which differs in detail from the one shown in this paper, is described by Mickley (12). Schmidt gave no examples and Mickley does not take an example to the point where results are obtained.

#### DERIVATIONS FOR GRAPHICAL METHOD

The graphical method of solution of Equation (5) is derived as follows. First, in order to remove  $f_2(y)$  from inside the differential, a change in variable is made:

$$dw = \pm \frac{dy}{f_2(y)} \quad (6)$$

In Equation (6) the sign may be selected for convenience in the particular problem. Then

$$\frac{\partial \phi}{\partial w} = \left( \frac{\partial \phi}{\partial y} \right) \left( \frac{dy}{dw} \right) = \pm f_2(y) \frac{\partial \phi}{\partial y} \quad (7)$$

and

$$\begin{aligned} \frac{\partial}{\partial y} \left( \frac{\partial \phi}{\partial w} \right) &= \left( \frac{dw}{dy} \right) \frac{\partial}{\partial w} \left( \frac{\partial \phi}{\partial w} \right) \\ &= \frac{1}{f_2(y)} \frac{\partial^2 \phi}{\partial w^2} \end{aligned} \quad (8)$$

Substitution of Equations (7) and (8) in Equation (5) gives

$$\frac{\partial \phi}{\partial x} = f_3(w) \left( \frac{\partial^2 \phi}{\partial w^2} \right) \quad (9)$$

when

$$f_3(w) = \frac{f_1(y)}{f_2(y)} \quad (10)$$

Equation (9), which is a linear partial-differential equation of simpler form than Equation (5), then is expressed in finite difference form. Partial derivatives are expressed as

$$\left( \frac{\partial \phi}{\partial x} \right)_{m,n} = \frac{\phi_{m+1,n} - \phi_{m,n}}{\Delta x} \quad (11)$$

and

$$\begin{aligned} \left( \frac{\partial^2 \phi}{\partial w^2} \right)_{m,n} &= \frac{1}{\Delta w_n} \left[ \frac{\phi_{m,n+1} - \phi_{m,n}}{\Delta w_{n+1/2}} \right. \\ &\quad \left. + \frac{\phi_{m,n-1} - \phi_{m,n}}{\Delta w_{n-1/2}} \right] \end{aligned} \quad (12)$$

The subscript  $m$  pertains to the coordinate  $x$  and subscript  $n$  pertains to coordinate  $w$ , as shown in Figure 2. Equation (11) is conventional, and the representation of the second derivative in Equation (12) is a logical extension of conventional formulas for the case in which unequal intervals of the independent variable are used. Equation (12) may be shown by Taylor's series expansion to be a correct representation using three unequally spaced points. The intervals of  $w$  are defined in Figure 2, in which it is seen that

$$\Delta w_n = \frac{1}{2} [\Delta w_{n+1/2} + \Delta w_{n-1/2}] \quad (13)$$

Substitution of Equations (11) and (12) in Equation (9) gives the equation

$$\begin{aligned} \phi_{m+1,n} - \phi_{m,n} &= \frac{(\Delta x) f_3(w_n)}{\Delta w_n} \left[ \frac{\phi_{m,n+1} - \phi_{m,n}}{\Delta w_{n+1/2}} \right. \\ &\quad \left. + \frac{\phi_{m,n-1} - \phi_{m,n}}{\Delta w_{n-1/2}} \right] \end{aligned} \quad (14)$$

Use of Equation (13) in Equation (14) leads to

$$\begin{aligned} \phi_{m+1,n} &= \left[ 1 - \frac{2(\Delta x) f_3(w_n)}{(\Delta w_{n+1/2})(\Delta w_{n-1/2})} \right] \phi_{m,n} \\ &\quad + \frac{(\Delta x) f_3(w_n)}{\Delta w_n} \left[ \frac{\phi_{m,n+1}}{\Delta w_{n+1/2}} + \frac{\phi_{m,n-1}}{\Delta w_{n-1/2}} \right] \end{aligned} \quad (15)$$

The finite increments in  $x$  and  $w$  are now constrained to satisfy the relationship

$$\frac{2(\Delta x) f_3(w_n)}{(\Delta w_{n+1/2})(\Delta w_{n-1/2})} = 1 \quad (16)$$

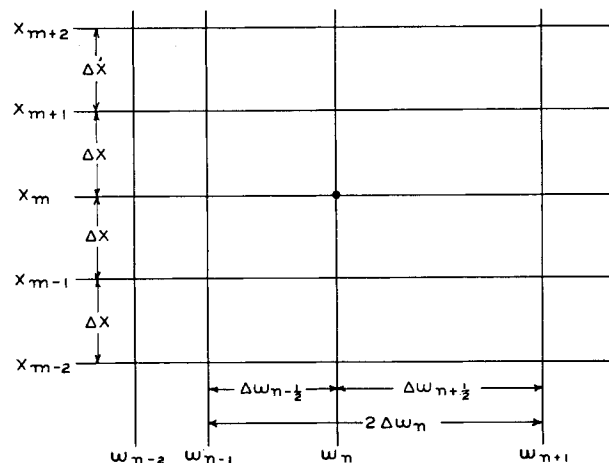


Fig. 2. Finite-difference grid.

If Equation (16) is substituted in Equation (15) and the result rearranged, the following is obtained:

$$\begin{aligned} \phi_{m+1,n} &= \frac{1}{2(\Delta w_n)} [(\phi_{m,n+1})(\Delta w_{n-1/2}) \\ &\quad + (\phi_{m,n-1})(\Delta w_{n+1/2})] \end{aligned} \quad (17)$$

Equation (17) is satisfied by the geometry of a Schmidt-type construction, as can be easily demonstrated in Figure 3 by use of the relationships for similar triangles.

The spacing of the discrete values of  $w$  is determined by solution of Equation (16). This solution must have appropriate numbers of intervals in both the  $x$  and  $w$  coordinates, and the size of the intervals in  $w$  should increase or decrease smoothly. Intervals must also be placed as required to establish boundary conditions.

The application of boundary conditions is similar to that with conventional

Schmidt plots. Boundary conditions of the type

$$\phi = \phi_a \text{ at } y = y_a \quad (18)$$

become

$$\phi = \phi_a \text{ at } w = w_a \quad (19)$$

where  $w_a$  is the value of  $w$  corresponding to  $y_a$ .

If

$$\frac{\partial \phi}{\partial y} = 0 \text{ at } y = y_a \quad (20)$$

use of Equation (7) gives

$$\frac{\partial \phi}{\partial w} = 0 \text{ at } w = w_a \quad (21)$$

as long as  $f_2(y_a)$  is finite. This boundary condition is imposed by imagining a mirror image on the other side of  $w_a$  and is illustrated in two examples which follow.

Another boundary condition which commonly arises owing to the finite thermal conductivity of a wall and to finite heat transfer coefficients is

$$\frac{\partial \phi}{\partial y} = C_1(\phi_a - \phi_s) \text{ at } y = y_a \quad (22)$$

With Equation (7) substituted, the boundary condition becomes

$$\frac{\partial \phi}{\partial w} = \pm C_1 f_2(y_a) [\phi_a - \phi_s] \text{ at } w = w_a \quad (23)$$

which is satisfied by the construction shown in Figure 4. A point at the level  $\phi_s$  is placed a distance  $1/C_1 f_2(y_a)$  measured in the units of  $w$  from  $w_a$  and is used as a constant-temperature point.

Extensions of the method to match other boundary conditions such as variable temperatures may be made.

#### USE OF GRAPHICAL METHOD

There follows an outline of the method of solution of a differential equation of the type shown by Equation (5).  $\phi$  is to be determined as a function of  $x$  and  $y$ , and it is presumed that the functions  $f_1(y)$  and  $f_2(y)$  are known in at least tabular form.

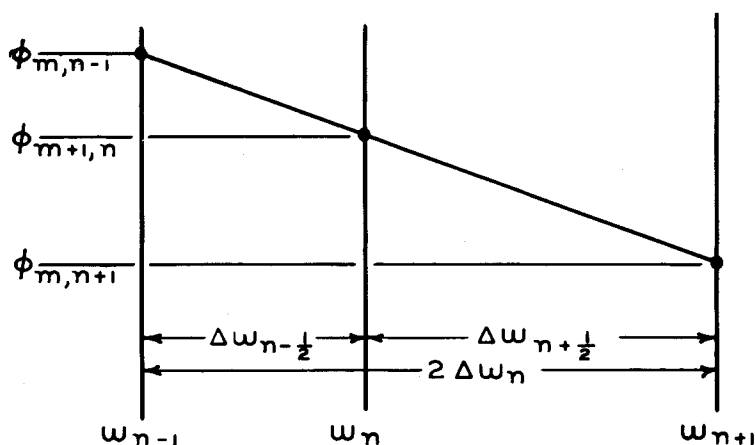


Fig. 3. Schmidt-type construction.

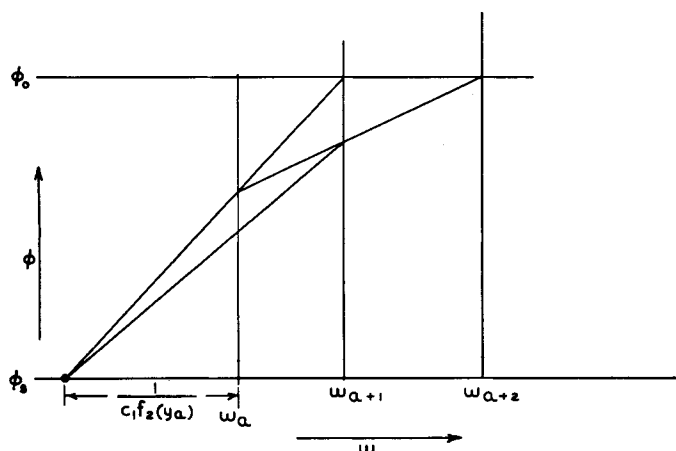


Fig. 4. Construction for boundary condition of Equation (23).

1. The new variable  $w$  should be calculated as a function of  $y$  by integration of Equation (6) between appropriate limits. This integration may well be done numerically or graphically.

2.  $f_3(w)$  as defined by Equation (10) is to be calculated as a function of  $y$  and, by use of the relationship obtained above between  $w$  and  $y$ ,  $f_3(w)$  should be plotted as a function of  $w$ .

3. Equation (16) and the graph of  $f_3(w)$  are used to calculate the intervals in  $w$ . In essence this amounts to writing Equation (16) for each interior point and, by trial and error, finding a set of  $w$  coordinates which satisfies the equation and has a suitable number of intervals. The solution can be systematized, however, so that the labor of obtaining such a set is not great. In the author's experience with this method there has always been evident a suitable place on the plot of  $f_3(w)$  at which to start the calculation. For Equation (1), if the velocity and eddy conductivity are symmetrical about the center line,  $f_3(w)$  will be likewise symmetrical, and a start is made at the center line by letting the intervals in  $w$  be symmetrical; that is, at the center line, Equation (16) becomes

$$(\Delta w_{n-1/2})^2 = 2(\Delta x)f_3(w_n) \quad (24)$$

A trial value of  $\Delta x$  is selected, and  $\Delta w$  for either side of the center line is calculated. Then, by use of Equation (16),  $\Delta w$ 's and therefore  $w$ 's are calculated step by step toward the wall. If, as is generally the case for a first iteration, the boundary does not coincide with a calculated  $w$ , the value of  $\Delta x$  is adjusted and the calculation repeated until a suitable value of  $\Delta x$  is found.

For Equation (3),  $f_3(w)$  goes to infinity at the center line of the pipe and also at the wall. In this case the minimum in  $f_3(w)$  is a suitable starting point, and the intervals  $\Delta w_{n-1/2}$  and  $\Delta w_{n+1/2}$  are taken as equal for  $w_n$  at this minimum. The procedure is illustrated in the examples below.

4. A graph of a size suitable for Schmidt-type constructions is made, with  $\phi$  as the ordinate and  $w$  as the abscissa. Vertical lines are drawn at the values of  $w$  calculated above. The boundary conditions are converted from the original form to those pertaining to  $\phi$  as a function of  $w$  and entered or used accordingly. A conventional Schmidt-type construction (7, 11) is then made. This is illustrated in Figure 5, which shows the construction for boundary conditions involving a step function in  $\phi$  at one boundary and  $(\partial \phi / \partial w)$  of zero at the second boundary, which might well be a center of symmetry. The value of  $\phi$  at the end of the fourth interval in  $x$  is shown dotted.

5. Values of  $\phi$  at the desired intervals of  $x$  are read as functions of  $w$  and converted to a basis of  $y$  by use of the plot of  $w$  vs.  $y$  previously made.

### Example 1. Heat Transfer with Laminar Flow and Parabolic Velocity Distribution

As a first example a fluid flowing in a laminar fashion in a pipe is considered. The velocity distribution is taken to be parabolic and invariant, and the fluid, which is at a uniform temperature  $T_0$ , enters a section having a wall temperature  $T_s$ . The temperature of the fluid as a function of position is desired.

The differential equation is

$$ru_x \frac{\partial T}{\partial x} = K \frac{\partial}{\partial r} \left[ r \frac{\partial T}{\partial r} \right] \quad (25)$$

with the boundary conditions

$$T = T_0 \quad \text{at} \quad 0 \leq r \leq r_0 \quad \text{for} \quad x < 0 \quad (26)$$

and

$$T = T_s \quad \text{at} \quad r = r_0 \quad \text{for} \quad x > 0 \quad (27)$$

The velocity distribution is given by

$$u_x = 2U \left[ 1 - \frac{r^2}{r_0^2} \right] \quad (28)$$

Dimensionless variables may be defined:

$$\eta = \frac{r}{r_0} \quad (29)$$

$$\phi = \frac{T - T_0}{T_s - T_0} \quad (30)$$

$$\lambda = \frac{Kx}{r_0^2 U} \quad (31)$$

Substitution of Equations (28) to (31) in Equations (25) to (27) gives

$$\frac{\partial \phi}{\partial \lambda} = \frac{1}{2\eta(1-\eta^2)} \frac{\partial}{\partial \eta} \left[ \eta \frac{\partial \phi}{\partial \eta} \right] \quad (32)$$

with boundary conditions

$$\phi = 0 \quad \text{at} \quad 0 \leq \eta \leq 1 \quad \text{for} \quad \lambda < 0 \quad (33)$$

and

$$\phi = 1 \quad \text{at} \quad \eta = 1 \quad \text{for} \quad \lambda > 0 \quad (34)$$

By symmetry a further boundary condition is known:

$$\frac{\partial \phi}{\partial \eta} = 0 \quad \text{at} \quad \eta = 0 \quad (35)$$

To prepare for graphical treatment, the change of variable shown in Equation (6) is used. For this case the change of variable becomes

$$dw = -\frac{d\eta}{\eta} \quad (36)$$

The negative sign was selected in order to make  $w$  positive. Integration of Equation (36) gives

$$w = -\ln \eta \quad (37)$$

The function defined by Equation (10) for this case is

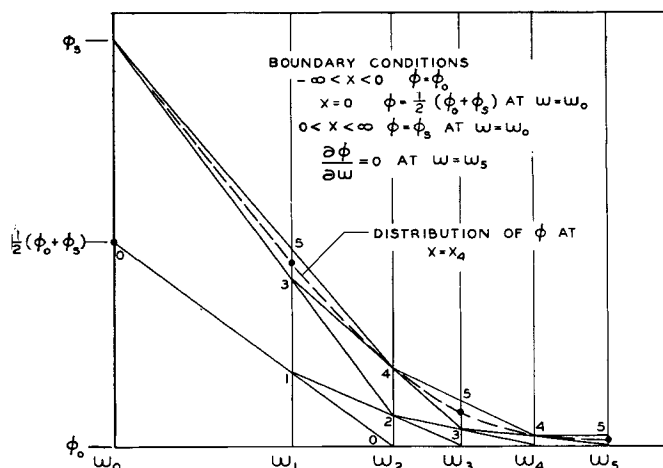


Fig. 5. Construction showing method of evaluating  $\phi$ .

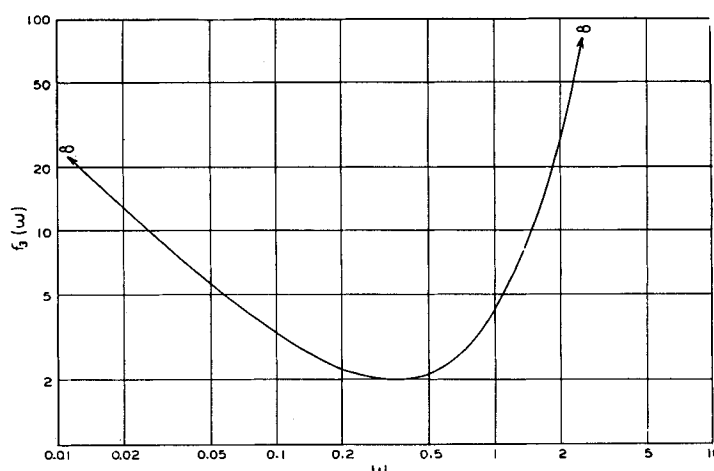


Fig. 6. The function  $f_3(w)$  in Example 1.

$$f_3(w) = \frac{1}{2\eta^2(1-\eta^2)} \quad (38)$$

Equations (37) and (38) were used to calculate  $w$  and  $f_3(w)$ , and in Figure 6,  $f_3(w)$  is shown as a function of  $w$ . As can be seen, a minimum in  $f_3(w)$  occurs at a  $w$  of about 0.35, and this was used as the starting point of calculations for the intervals  $\Delta w$ . A value of  $2.66 \times 10^{-3}$  for  $\Delta \lambda$  was found, by trial, to be satisfactory in that an interval ended at  $w = 0$  and that a suitable number of intervals  $\Delta w$  were formed. With this value of  $\Delta \lambda$  Equation (24) becomes

$$(\Delta w_{n-1/2})^2 = 2(\Delta \lambda) f_3(w_n) = 0.01064 \quad (39)$$

which applies only for  $w_n$  corresponding to the minimum value of  $f_3(w)$ . Equation (16), which applies everywhere, becomes

$$(\Delta w_{n+1/2})(\Delta w_{n-1/2}) = 5.32 \times 10^{-3} f_3(w_n) \quad (40)$$

The values of  $w_n$  which satisfy these equations and the corresponding values of

$\eta_n$  have been tabulated (10). Since the transformation of Equation (37) has the characteristic that

$$w \rightarrow \infty \quad \text{as} \quad \eta \rightarrow 0 \quad (41)$$

the intervals are not extended to  $\eta = 0$ ; however since  $\eta$  can be made as small as is desired, no real difficulty is introduced. In this case a minimum value of  $\eta$  of 0.0348, with fifteen intervals, was deemed adequate.

The boundary conditions must be expressed in terms of  $w$ . These are

$$\phi = 0 \quad \text{at} \quad 0 \leq w < \infty \quad \text{for} \quad \lambda < 0 \quad (42)$$

$$\phi = 1 \quad \text{at} \quad w = 0 \quad \text{for} \quad \lambda > 0 \quad (43)$$

and

$$\frac{\partial \phi}{\partial w} \rightarrow -0 \quad \text{as} \quad w \rightarrow \infty \quad (44)$$

The boundary conditions of Equations (42) and (43) are easily handled, and the one of Equation (44) is approximated in this case by

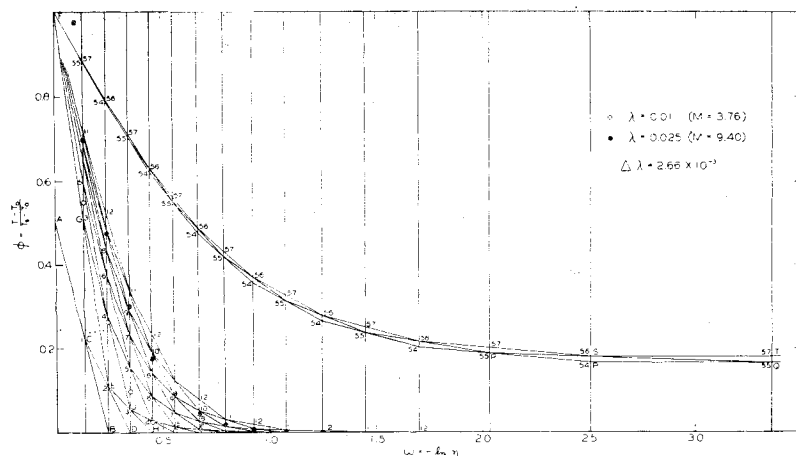


Fig. 7. Graphical construction for Example 1.

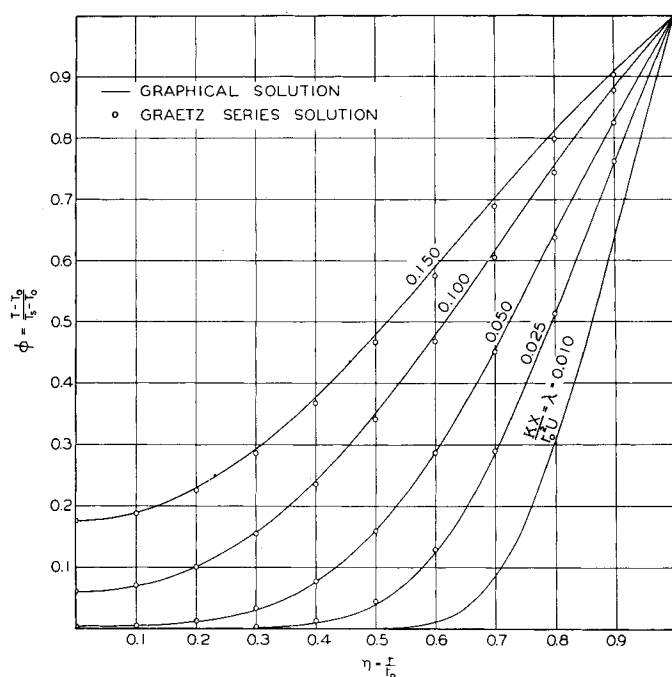


Fig. 8. Solutions for Example 1.

$$\frac{\partial \phi}{\partial w} = 0 \quad \text{at} \quad w = 3.36 \quad (45)$$

A Schmidt-type plot was made of  $\phi$  against  $w$  on large cross-section paper, and vertical lines were entered at the values of  $w$  calculated by use of Equation (40). Figure 7 is a reproduction of this plot showing the spacing of the lines and the construction for the first few intervals  $\Delta\lambda$ . The boundary condition for  $\lambda = 0$  is interpreted as  $\phi = 0.5$  at the boundary  $w = 0$ , since this is the average of the values of  $\phi$  for  $\lambda < 0$  and  $\lambda > 0$ . Construction is started by drawing a line between the points labeled A and B, which are conditions at  $\lambda = 0$ . The condition at  $\Delta\lambda$  is given by point C, in accordance with Equation (17) and Figure 3. Construction of the line CD gives point E as a condition at  $2\Delta\lambda$ . Since point F represents the condition at the boundary for  $\lambda > 0$  it is now

used, and lines EF and EH are drawn, points G and J being given as points for  $3\Delta\lambda$ . The numbers at the points in Figure 6 correspond to  $M$  in the equation

$$\lambda = M\Delta\lambda \quad (46)$$

The construction for a few intervals at higher values of  $\lambda$ ,  $M = 55, 56$ , and  $57$ , is shown to illustrate the treatment of the boundary condition of Equation (45). The points at  $M = 54$  are from previous construction. For  $M = 55$  a horizontal line is drawn from P intersecting the line  $w = 3.36$  at Q, which becomes the value for  $M = 55$ . This construction satisfies the boundary condition of Equation (45). Point S, for  $M = 56$ , is obtained conventionally by drawing a line between R and Q, and point T, for  $M = 57$ , is again obtained by drawing a horizontal line, this time from point S.

Points interpolated for two even values

of  $\lambda$ , 0.01 and 0.025, are indicated on Figure 7. The numerical values of  $\phi$  found for even values of  $\lambda$  are available (10).

## COMPARISON WITH ANALYTIC SOLUTION

The results of this graphical solution of the differential Equation (25), as described above, are shown in Figure 8. Graetz (6) found an analytic solution to this problem which is described by Jakob (7) and others. The temperature is expressed as an infinite series for which the coefficients of only the first few terms are known. If the dimensionless variables of Equations (29) through (31) are used, the Graetz solution as given by Jakob is

$$\begin{aligned} \phi = & 1 - 1.477e^{-3.658\lambda}R_0(\eta) \\ & + 0.810e^{-22.178\lambda}R_1(\eta) \\ & - 0.385e^{-53.05\lambda}R_2(\eta) + \dots \quad (47) \end{aligned}$$

whereas Lee, Nelson, Cherry, and Boelter (9) give

$$\begin{aligned} \phi = & 1 - 1.476e^{-3.656\lambda}Y_1(\eta) \\ & + 0.807e^{-22.305\lambda}Y_2(\eta) \\ & - 0.589e^{-56.956\lambda}Y_3(\eta) \\ & + 0.479e^{-107.619\lambda}Y_4(\eta) - \dots \quad (48) \end{aligned}$$

Equation (48) has one more term of the series than does Equation (47). The coefficients and exponents are somewhat different in these two equations, as are also the functions  $R_n$  and  $Y_n$  as tabulated by the respective authors. The truncated series is not useful for low values of  $\lambda$ , since it converges too slowly and is reported (8) as being invalid for  $\lambda < 0.03$ .

Points calculated by use of Equation (48) are shown for four values of  $\lambda$  in Figure 8. Equation (48) was selected instead of (47), because Equation (47) was found to diverge from the graphical solution for  $\lambda = 0.05$ . Both equations gave essentially identical results for  $\lambda = 0.10$  and  $0.15$ . Points for values of  $r/r_0$  of less than 0.3 are not shown for  $\lambda = 0.025$ , because these values oscillate about zero and would cause confusion.

Agreement between the graphical solution and the Graetz series solution is seen to be very good for  $\lambda = 0.025$  and  $\lambda = 0.05$ . For  $\lambda = 0.10$  and  $\lambda = 0.15$  there are some differences, although central temperatures agree. The maximum deviation of a point from the graphical solution is 0.014 in terms of  $\phi$ , occurring for  $\eta = 0.7$  and  $\lambda = 0.15$ . This accuracy is considered more than adequate for engineering purposes.

## Example 2. Heat Transfer with Turbulent Flow

Heat transfer to a turbulently flowing liquid is treated as a second example of the application of this graphical method of solution of the governing differential equations. The problem selected concerns water, initially at a uniform temperature of 200°F., flowing with a bulk velocity of 10 ft./sec. in a pipe 4.00 in. in internal diameter. The water enters a section of heated copper pipe having a wall thickness of 0.25 in. Saturated steam at an absolute pressure of 25 lb./sq. in. is condensing on the exterior of the pipe with a heat transfer coefficient

of 3,000 B.t.u./(hr.)(sq. ft.)(°F.). The radial temperature distributions in the water at positions 5, 10, and 15 ft. from the entrance to the heated section are desired. It is assumed that fully developed turbulence exists at the entrance section.

Equation (3) is the differential equation describing this situation. Boundary conditions are

$$T = 200^\circ F. \quad \text{for } 0 \leq r \leq r_0 \quad (49)$$

at  $x < 0$

$$T_s = \text{temp. steam} = 240^\circ F. \quad (50)$$

for  $x > 0$

and by symmetry

$$\frac{\partial T}{\partial r} = 0 \quad \text{at } r = 0 \quad (51)$$

The functions for the general form of Equation (5) are

$$f_1(r) = \frac{1}{u_x r} \quad (52)$$

$$f_2(r) = r \epsilon_c \quad (53)$$

and

$$f_3(w) = \frac{1}{u_x r^2 \epsilon_c} \quad (54)$$

The variable  $w$  is defined by

$$dw = -\frac{dr}{r \epsilon_c} = +\frac{d(r_0 - r)}{r \epsilon_c} \quad (55)$$

Before Equations (54) and (55) can be applied, the velocity distribution and the point values of the total conductivity must be known. The velocity distribution was estimated by use of the relationships (4)

$$u^+ = \frac{1}{0.0695} \tanh(0.0695r^+) \quad (56)$$

for  $r^+ \leq 26.7$

$$u^+ = 5.5 + 2.5 \ln r^+ \quad (57)$$

for  $r^+ > 26.7$

The eddy viscosity was determined by use of

$$\frac{\epsilon_m}{\nu} = \frac{r}{r_0} \cosh^2 [0.0695r^+] \quad (58)$$

for  $r^+ \leq 26.7$

$$\frac{\epsilon_m}{\nu} = 0.4 \frac{r}{r_0} r^+ \quad (59)$$

for  $r^+ > 26.7$

Because the Reynolds number is very high,  $10^6$ , the eddy conductivity was determined by use of the approximation

$$Pr_{eddy} = \frac{\epsilon_m}{\epsilon_c} = 1 \quad (60)$$

The calculated values of the velocity, the total conductivity, the new variable  $w$ , and the function  $f_3(w)$  were tabulated (10) as functions of the radius. Figure 9 shows

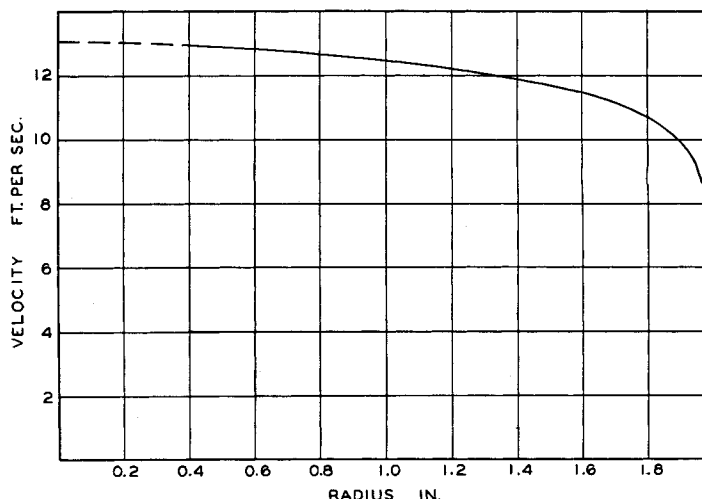


Fig. 9. Velocity distribution for Example 2.

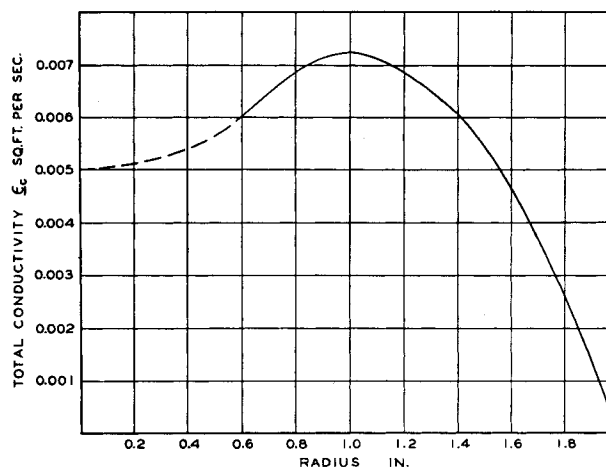


Fig. 10. Total conductivity for Example 2.

the estimated velocity distribution, the dotted portion representing a departure from Equation (57), because the latter erroneously gives a nonzero slope at the center line. The estimated total conductivity is shown in Figure 10, in which the dotted portion represents a departure from values calculated by use of Equations (59) and (60), because the eddy conductivity is known (4) to remain fairly large near the center of the channel. In Figure 11 the variable  $w$  is shown as a function of the radius deficiency ( $r_0 - r$ ). The behavior of the function  $f_3(w)$  is shown in Figure 12, in which it is plotted as a function of  $w$ . A minimum in  $f_3(w)$  occurs at a value of  $w$  of 505 sec./sq. ft.

Solution for a suitable set of values of  $w$  was carried out by use of Equation (24) for the value of  $w$  of 505 sec./sq. ft. and Equation (16) for the other values of  $w$ . By trial, a value of  $\Delta x$  of 0.569 ft. was found to give ten intervals, which was considered appropriate, including an interval ending at  $w = 0$ .

The boundary condition of Equation (50) leads to an equation of the form of Equations (22) and (23). If conduction in

the metal wall parallel to the axis is neglected, the thermal flux from the steam may be equated to that through the wall and to that entering the water:

$$\left(\frac{\partial T}{\partial r}\right)_{r_0} = \frac{T_s - T_{r_0}}{(\sigma C_P \epsilon_c) r_0 \left[ \frac{r_0}{hr_1} + \frac{r_0}{k_m} \ln \frac{r_1}{r_0} \right]} \quad (61)$$

Use of Equations (23) and (53) with Equation (61) shows that the construction distance in  $w$  units is

$$\frac{1}{C_1 f_2(r_0)} = (\sigma C_P) \left[ \frac{1}{r_1 h} + \frac{1}{k_m} \ln \frac{r_1}{r_0} \right] \quad (62)$$

which was found to be 502 sec./sq. ft.

A large-scale plot was made on cross-section paper with temperature as the ordinate and  $w$  as the abscissa. Vertical lines were drawn at the calculated values of  $w$  (10) and the graphical solution was performed. Figure 13 is a reproduction of this plot showing the construction. The construction for the  $\Delta x$  intervals 9 through 26 is omitted in the interest of clarity. The points are numbered to correspond to  $M$  in

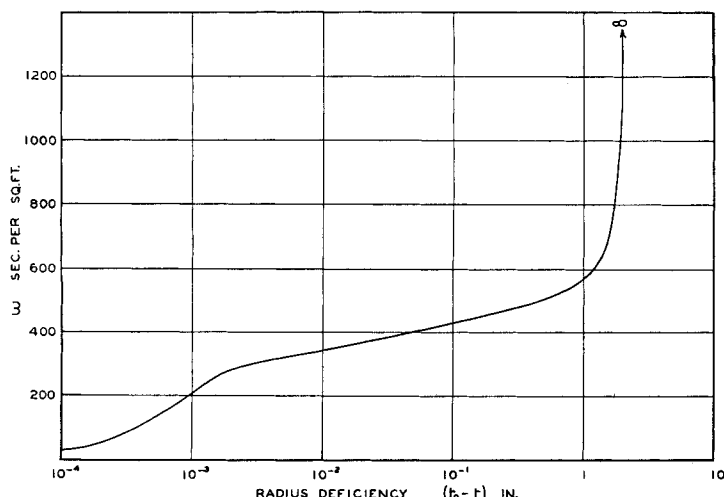


Fig. 11. Transformation variable  $w$  for Example 2.

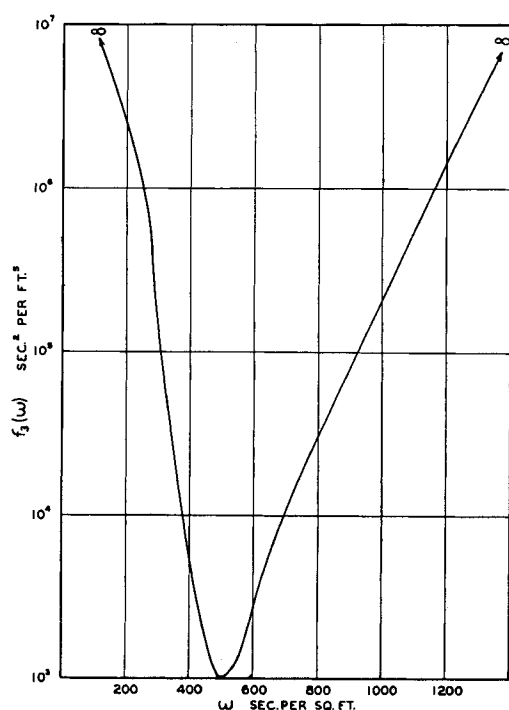


Fig. 12. Function  $f_3(w)$  for Example 2.

$$x = M\Delta x \quad (63)$$

Values of the radius are indicated at the top of Figure 13 in order to show the extreme variation in the intervals of radius which are used to satisfy the equations governing the graphical solution.

The temperatures for the downstream distances of 5, 10, and 15 ft. (10) were read from Figure 13. The temperature distributions for bulk of the stream are shown in Figure 14 and the distributions close to the wall are presented in Figure 15.

## DISCUSSION

The procedure demonstrated is a straightforward method of solving differential equations of the form of Equation (5). The method does not require special-

ized equipment such as analogue or digital computers or excessive amounts of time.

The examples selected were taken from the field of heat transfer to flowing fluids, but the derivations of Equations (6) through (24) are more general and the method may well be applied to any differential equation which can be expressed in the form of Equation (5). The examples demonstrate that no undue difficulty is caused by enormous variation in the functions  $f_1(y)$  and  $f_2(y)$ .

The method is demonstrated as a graphical one and indeed the graphical solution appears advantageous. There may be situations, however, in which a numerical solution is to be preferred. Numerical solution can be accomplished

by use of Equation (17), the weighting factors of which can be calculated for each interval in  $w$  and then used to evaluate values of  $\phi$ .

## ACKNOWLEDGMENT

The assistance of W. N. Lacey in reviewing the manuscript is gratefully acknowledged.

## NOTATION

- $C_1$  = a constant
- $c_k$  = concentration of component  $k$ , (lb.)/(cu. ft.)
- $C_p$  = specific heat at constant pressure, B.t.u./(lb.)(°F.)
- cosh = hyperbolic cosine
- $D_{ky}$  = Fick diffusion coefficient for component  $k$  in  $y$  direction
- $d$  = differential operator
- $e$  = base of natural logarithms, 2.71828—
- $f$  = Fanning friction factor
- $f_1(y)$  = function of  $y$  [Equation (5)]
- $f_2(y)$  = function of  $y$  [Equation (5)]
- $f_3(w)$  =  $f_1(y)/f_2(y)$
- $h$  = heat transfer coefficient, B.t.u./(sq. ft.)(sec.)(°F.)
- $k_m$  = thermal conductivity of wall, B.t.u./(ft.)(sec.)(°F.)
- ln = natural logarithm
- $M$  = number of intervals in  $x$  or  $\lambda$
- $\dot{m}$  = weight rate of transport, lb./(sq. ft.)(sec.)
- $Pr$  = Prandtl number
- $\dot{Q}$  = thermal flux, B.t.u./(sq. ft.)(sec.)
- $R_n$  = coefficient in Graetz series given by Jakob (7)
- $r$  = radius, ft.
- $r^+$  = distance parameter  $(r_0 - r)U\sqrt{f/2\nu}$
- $r_0$  = internal radius of pipe, ft.
- $r_1$  = external radius of pipe, ft.
- $T$  = temperature, °F.
- $T_0$  = original temperature of fluid, °F.
- $T_s$  = temperature at one boundary, °F.
- tanh = hyperbolic tangent
- $U$  = gross velocity, ft./(sec.)
- $u$  = point velocity, ft./(sec.)
- $u^+$  = velocity parameter  $u/U\sqrt{f/2}$
- $w$  = transformation variable (varying units)
- $x$  = Cartesian coordinate in direction of flow, ft.
- $Y_n$  = coefficient in Graetz series given by Lee et al. (9)
- $y$  = generalized distance coordinate; Cartesian coordinate, ft.
- $z$  = Cartesian coordinate, ft.
- $\Delta$  = increment in
- $\epsilon_e$  = eddy conductivity, sq. ft./sec.
- $\epsilon_o$  = total conductivity,  $(\epsilon_e + K)$ , sq. ft./sec.
- $\epsilon_D$  = eddy diffusivity, sq. ft./sec.
- $\epsilon_D$  = total diffusivity,  $(\epsilon_D + D)$ , sq. ft./sec.
- $\epsilon_m$  = eddy viscosity, sq. ft./sec.
- $\epsilon_m$  = total viscosity,  $(\epsilon_m + \nu)$ , sq. ft./sec.

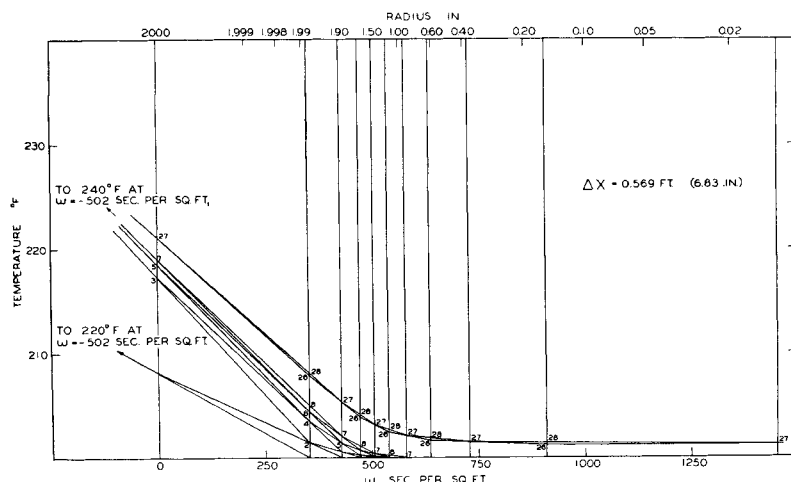


Fig. 13. Graphical construction for Example 2.

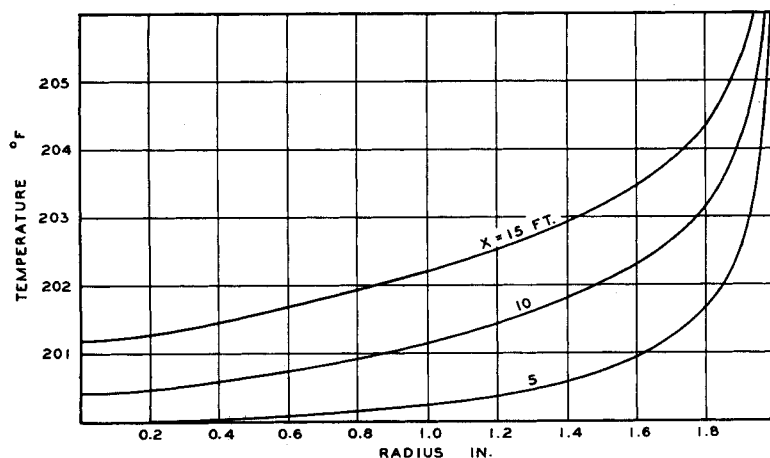


Fig. 14. Temperature distributions determined in Example 2.

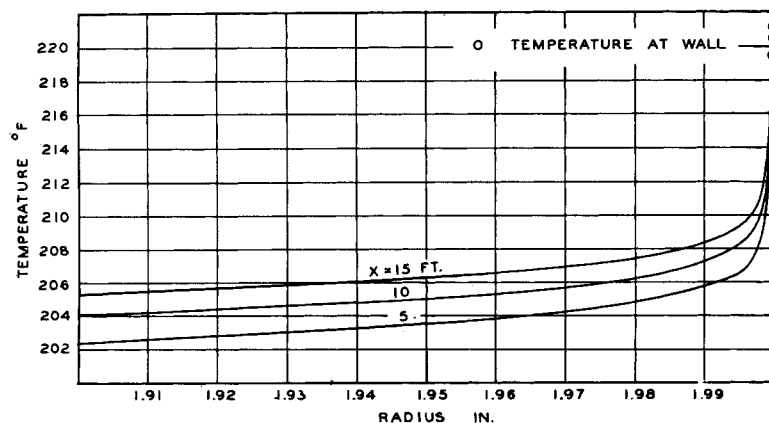


Fig. 15. Temperature distributions close to wall in Example 2.

- $\eta = r/r_0$   
 $K =$  thermometric conductivity, sq. ft./sec.  
 $\lambda = Kx/r_0^2 U$   
 $\nu =$  kinematic viscosity, sq. ft./sec.  
 $\sigma =$  specific weight, lb./cu. ft.  
 $\phi =$  dependent variable; also  $(T - T_0)/(T_s - T_0)$   
 $\partial =$  partial-differential operator

#### Subscripts

- $a =$  boundary  
 $k =$  diffusing component  
 $m =$  intervals in  $x$  or  $\lambda$  direction  
 $n =$  intervals in  $y$ ,  $r$  or  $w$  direction  
 $0 =$  bulk condition at  $x = 0$   
 $r =$  radial direction  
 $s =$  boundary condition  
 $x, y = x, y$  directions

#### LITERATURE CITED

- Berry, V. J., *Appl. Sci. Research (A)*, **4**, 61 (1953).
- Butler, R. M., and A. C. Plewes, *Chem. Eng. Progr. Symposium Ser. No. 10*, **50**, 121 (1954).
- Carslaw, H. S., and J. C. Jaeger, "Conduction of Heat in Solids," Clarendon Press, Oxford (1947).
- Corcoran, W. H., and B. H. Sage, *A.I.Ch.E. Journal*, **2**, 251 (1956).
- Graetz, L., *Ann. Physik*, **18**, 79 (1883).
- Ibid.*, **25**, 337 (1885).
- Jakob, Max, "Heat Transfer," vol. I, John Wiley and Sons, Inc., New York (1949).
- Kays, W. M., *Tech. Report No. 20*, Contract N60NR-251, T.O.6, Stanford Univ., Stanford, Calif. (1953).
- Lee, A., W. O. Nelson, V. H. Cherry, and L. M. K. Boelter, *Proc. Fifth Internatl. Congress Appl. Mech.*, p. 571, (1938).
- Longwell, P. A., Document 5304, American Documentation Institute Auxiliary Publications Project, Library of Congress, Washington 25, D. C., \$1.25 for photostat or 35-mm. microfilm.
- McAdams, W. H., "Heat Transmission," 3 ed., McGraw-Hill Book Company, Inc., New York (1954).
- Mickley, H. S., T. K. Sherwood and C. E. Reed, "Applied Mathematics in Chemical Engineering," 2 ed., McGraw-Hill Book Company, Inc., New York (1957).
- Nessi, A., and L. Nissolle, "Méthodes Graphiques pour l'étude des Installations de Chauffage et de Réfrigération en Régime Discontinu," Dunod, Paris (1929).
- Norris, R. H., and D. D. Streid, *Trans. Am. Soc. Mech. Engrs.*, **62**, 525 (1940).
- Opfell, J. B., and B. H. Sage, *Ind. Eng. Chem.*, **47**, 918 (1955).
- Schlenger, W. G., V. J. Berry, J. L. Mason, and B. H. Sage, *Ind. Eng. Chem.*, **45**, 662 (1953).
- Schmidt, E., "Festschrift zum Siebzigsten Geburtstag August Foepppls," p. 179, Julius Springer, Berlin (1924).
- , *Forsch. Gebiete Ingenieur.*, **13**, 177 (1942).
- Schenk, J., *Appl. Sci. Research (A)*, **5**, 241 (1955).